

Received October 7, 2017, accepted November 8, 2017, date of publication November 29, 2017, date of current version February 14, 2018.

Digital Object Identifier 10.1109/ACCESS.2017.2778022

# A PSO Optimization Scale-Transformation Stochastic-Resonance Algorithm With Stability Mutation Operator

LING TONG<sup>1</sup>, XIAOGANG LI<sup>2,3</sup>, JINHAI HU<sup>3</sup>, AND LITONG REN<sup>3</sup>

<sup>1</sup>Xi'an International Studies University, Xi'an 710128, China

<sup>2</sup>College of Aeronautics, Northwestern Polytechnical University, Xi'an 710072, China

<sup>3</sup>Air Force Engineering University, Xi'an 710038, China

Corresponding author: Ling Tong (tongling@xisu.edu.cn)

This work was supported in part by the Natural Science Foundation of China State Natural Science Foundation under Grant 51105374, in part by the Aeronautical Science Foundation of China under Grant 20142196019 and in part by the Natural Science Basic Research Plan in Shaanxi province of China under Grant 2015JM5207

**ABSTRACT** When using the PSO (particle swarm optimization) optimization adaptive stochastic-resonance method, the initial value and value range of the optimization parameters are defined inappropriately, divergence problems may easily emerge in the calculation process, and optimization may stop prematurely. To solve this problem, this research has analyzed the parameters that influence system stability using the scale-transformation stochastic-resonance solution procedure, and the value range leading to algorithm stability was obtained. On this basis, a stable mutation operator has been proposed, which is used in mutation operations on particles outside the stable condition. To ameliorate the poor local search ability and low convergence speed of the PSO algorithm in the later iteration stage, an inertial weight degression strategy based on a particle distance index has been developed. Based on these two research results, a PSO optimization scale-transformation stochastic-resonance algorithm with mutation operator has been proposed. The proposed algorithm has been used to detect numerically simulated signals and rotor test-table data. The results show that when the stable mutation operator acts on the SR optimization parameters, divergence is effectively avoided, and the stability of the iterative algorithm is improved accordingly. By adding the inertial weight degression strategy to the PSO algorithm, iteration speed could be improved at the same time.

**INDEX TERMS** Fault detection, particle swarm optimization (PSO), scale-transformation stochastic resonance, signal processing, stability analysis.

## I. INTRODUCTION

When faults occur in the rotors of aero-engines, their status is always reflected by vibration signals [1]. These vibration signals present different frequency characteristics for each different fault status. Therefore, vibration analysis is a common and effective method for aero-engine fault diagnosis. During practical use of this method, the vibration signals detected by sensors always contain high-energy noise which arises from the working environment. To solve this problem, various methods or algorithms are used to reduce or filter the noise, thus boosting the signal-to-noise ratio (SNR). However, when the noise is weakened, the fault signal is also influenced, and therefore it will be difficult to obtain an ideal fault-detection result. Moreover, the sensor detects the vibration signals from the whole engine. The exciting force induced by the rotors' unbalanced weight is the main

reason that the engine vibrates [1]. Under this condition, if the fault signal is somewhat weak, the fault characteristic may be inconspicuous compared to the inherent vibration of the engine. Therefore, a reasonable analysis method is needed to detect the main fault feature, thus achieving an ideal fault-detection result.

As a signal processing method, the stochastic-resonance (SR) method is different from traditional methods which improve the signal-to-noise ratio by reducing or modifying noise [2], [3]. The SR method uses the properties of a special nonlinear bistable system. When a signal acts on the system, the noise in the signal will exert an impelling effect. Then the periodicity of the output signal can be enhanced, and the SNR will rise accordingly. With this method, the useful signals will not be weakened, which always happens when traditional filtering algorithms are used.

However, classical SR theory is based on the adiabatic approximation theory, which restricts the theory to detection of small signals. To expand the theory to a larger scale, researchers have proposed scale-transformation stochastic resonance [3], sliding-window stochastic resonance [4], parameter-tuning stochastic resonance [5], and similar methods, with acceptable processing results. According to stochastic theory [6], the best stochastic-resonance state can be achieved only when the signal and noise intensities reach a sort of matching state. However, the signal and the noise are both unknown in practice, making the matching state difficult to achieve. To solve this problem, different adaptive optimization methods are used to tune the SR parameters adaptively, with the aim of achieving the ideal SR effect.

Asdi *et al.* proposed an adaptive stochastic-resonance algorithm based on a signal-to-noise ratio index, which achieved improved detection performance for short-length data [7]. Mitaim from the University of Southern California defined the adaptive stochastic-resonance algorithm systematically [8]. His research aimed to find an appropriate type of noise to match a given type of signal, in the expectation that the best SR result could be obtained under the optimal noise ratio. In addition, an adaptive stochastic-resonance system was designed in this work. However, the situation with unknown signal and noise was not addressed.

Since parameter-tuning stochastic resonance was proposed, researchers have preferred to realize adaptive SR by tuning the parameters. Ye *et al.* [9] obtained a set of optimal system parameters using noise intensity, signal frequency, and the proportional relationship between system parameters and standard SR. The analytical result was used to design an adaptive SR method. When the system is in its best SR state, the output SNR will reach its maximum. Based on this phenomenon, Yang *et al.* constructed an adaptive SR algorithm using the SNR and a linear random search algorithm which was used for periodic signal detection [10]. To overcome the limitation of sampling SR twice for large parameters, Deng *et al.* [11] proposed an SR method that could tune the sampling frequency and system parameters automatically based on the cooperative relation between signal, noise, and system. Zhao and Guo [12] researched system change trends in different frequency ranges according to the relationship between system outputs and parameters. An adaptive parameter-tuning SR method for nonlinear bistable systems was proposed. Xu *et al.* [13] regarded the highest peak in the output frequency spectrum as the signal frequency. Then the output SNR was chosen as the optimization parameter, and a genetic algorithm optimizing the SR method was proposed and used for varying-amplitude signal detection. Huang *et al.* [14] realized single-parameter optimizing SR control, which took the power spectrum as the optimization index. Tan *et al.* [15] took the highest spectrum-peak location and zero distance variance as the optimization index, thus offsetting the disadvantage that SNR needs to have the accurate signal frequency. Then the periodic signal

and the system were used to obtain the optimal match status using the mesh optimization algorithm. The proposed method was used for weak signal detection. Shen *et al.* [16] performed recovery of noisy mixed pictures by tuning the bistable system parameters]. Mutual information entropy was chosen as the optimization index. Zhu *et al.* [17] investigated the influence of adaptive coupling intensity on an SR system based on a small-world network connection. Wang *et al.* proposed a combination of a genetic algorithm and a frequency-shift scale-transformation stochastic-resonance method, with the system parameters  $a$  and  $b$  optimized synchronously. Adaptive detection under large-parameter conditions was achieved [18]. In [19], the output SNR was chosen as the target value. To change the barrier height, a genetic algorithm was used to tune  $a$  and  $b$  dynamically, and the optimal stochastic-resonance result was obtained. Also in this research, the best parameter curves for three parameter-setting methods were compared, showing that when the noise changes significantly, setting  $a$  and  $b$  together will be more favorable. An adaptive cascade stochastic-resonance method has been proposed in [20]. The method, which was described earlier, was based on the correlation coefficient of input signal and noise. A weighted SNR value was taken as the optimization index, thus avoiding the effect of unknown signals on the stochastic-resonance result. Li *et al.* [21] combined particle swarm optimization (PSO) and scale transformation and chose the weighted kurtosis index as the fitness function. The method was used to detect impact signals.

According to this literature analysis, the existing SR methods focus mainly on selecting appropriate optimization parameters and fitness functions to achieve an ideal SR result. However, the intensities of the actual signal and the noise are both nonadjustable when under detection. Consequently, the system parameters are widely used as the tuning object in adaptive SR methods designed for practical signals. The most commonly used optimization parameters are the system parameters  $a$  and  $b$ , as well as the frequency compression ratio  $R$  in scale-transformation stochastic resonance. During the application process, it has been found that divergence always occurs when the parameters are being optimized. A literature review revealed that very few relevant papers have analyzed this problem. After study of the solution procedure, it was found that when the Runge-Kutta method is used to solve the Langevin equation, parameters  $a$ ,  $b$ , and  $R$  participate in the iteration process directly or indirectly. If the initial value is inappropriate or the random value during the optimization process is too large, the iteration cannot converge, and the stability of the SR algorithm will be impacted accordingly.

The adaptive SR method also encounters divergence problems due to inappropriate selection of initial values and ranges for the optimization parameters. To solve this problem, a PSO optimization scale-transformation stochastic-resonance algorithm with mutation operator has been proposed in this article.

In the present paper, the basic theory of the classical SR algorithm and the scale-transformation SR algorithm

are introduced in Section II. Then, according to the scale-transformation SR solution process, an analysis of the effect of various parameters on system stability was conducted, and the value range of  $R$  that could confirm stability was obtained, as described in Section III. The theory of particle swarm optimization is presented at the beginning of Section IV. To overcome the algorithm's inadequacies in local search, an inertial weighted convergence strategy based on particle distance has been proposed. The stability analysis result presented in Section III has been used to construct a stable mutation operator. On this basis, a PSO optimization scale-transformation stochastic-resonance algorithm is proposed. Section V describes the use of numerical signal and rotor test-table data to test the detection results of the proposed algorithm. Finally, conclusions are drawn in Section VI.

## II. THEORETICAL BACKGROUND

### A. CLASSIC STOCHASTIC-RESONANCE THEORY

The Langevin equation of classic stochastic resonance can be written as [3]:

$$\dot{x} = -\dot{U}(x) + s(t) + n(t) \quad (1)$$

where  $U(x)$  is the bistable potential function

$$U(x) = -\frac{1}{2}ax^2 + \frac{1}{4}bx^4 \quad (2)$$

where  $a$  and  $b$  are the system parameters, which are greater than one,  $s(t)$  are the input signals, and  $n(t)$  is noise. The mean value is zero, and the noise intensity is  $D$ .

The bistable system has two stable states:  $x_{1,2} = \pm\sqrt{a/b}$  and a critical stable state  $x_3 = 0$ . The barrier height is  $\Delta U = a^2/4b$ . When the periodic signal is added to the system, assume that the signal frequency is  $f_0$  and the amplitude is  $A$ , which is greater than the critical value  $A_c = \sqrt{4a^3/27b}$ . Driven by the signal, the stable value will move to unequal status as a result. The stable value will rise and fall periodically with frequency  $f_0$ . Noise can achieve the same arousal effect. The transition movement can be judged by the mean transition ratio  $r_K$ .

Researches [22] has shown that when the periodic signal is mixed with noise, state transition will occur even though the signal amplitude  $A \ll A_c$ . This phenomenon is the foundation of classical stochastic resonance. The bistable system is under the combined influence of a weak periodic signal and strong noise; the stable value will change periodically. The transition movement has the same frequency as the periodic signal. Consequently, the system output will reflect the frequency characteristics of the input signal, which will achieve the goal of weak signal detection.

### B. SCALE-TRANSFORMATION STOCHASTIC RESONANCE

Limited by the adiabatic approximation theory, classical stochastic resonance is only appropriate for signals with frequency much less than one. This situation has restricted the application range of stochastic resonance. Taking an aviation engine as an example, the rotation speed in cruise state

reaches about  $12000r/\text{min}$ . This means that the rotation frequency is already  $200\text{Hz}$ . At the same time, the gears and bearings possess transmission relationships with the engine rotors, and their frequency also reaches scores of Hertz. Because the signal is a large-parameter signal, if classical stochastic resonance is applied directly, it will be impossible to achieve an ideal result.

Scale-transformation stochastic resonance can perform linear compression on the signal by resampling. This method can transform the large-frequency signal into a series of small-frequency ones, thus satisfying the requirements of stochastic resonance. Then the characteristic frequency can be obtained through spectrum analysis. The signal's actual frequency is obtained after signal scale reduction. To use this method, the frequency compression ratio  $R$  must first be determined. Then the second sampling frequency  $f_s$  is computed using  $R$ . Thus, the new sampling step length is  $h = 1/f_s r$ . The resampled signal is imported into the bistable system, and the actual characteristic frequency can then be determined through spectrum analysis on the output signal and scale reduction.

### III. STABILITY ANALYSIS OF THE SR ALGORITHM

When processing vibration signals with the stochastic-resonance method, the results are usually sensitive to the chosen system parameters. Therefore, the self-adaptive stochastic-resonance method is commonly used to process real vibration signals. When choosing optimization parameters, it is best to concentrate on the system parameters  $a$ ,  $b$  as well as the frequency compression coefficient  $R$  of the scale-transformation stochastic-resonance algorithm. It is known from the definition of the potential barrier,  $\Delta U = a^2/4b$ , that the system parameters  $a$ ,  $b$  determine the barrier height of the particle transition, while the output result is finally influenced by the value of  $\Delta U$ . Seen from this angle, singly optimizing one parameter ( $a$  or  $b$ ) while fixing the other has the same effect as optimizing  $a$ ,  $b$  at one time. To reduce the number of parameters to be optimized, in this paper,  $a$  has been set to one when changing the barrier height of the bistable system  $\Delta U$  through adjusting the value of  $b$  to obtain the optimal stochastic-resonance result.

However, has it not been found by analysis of the SR iteration process that because the equation is nonlinear, the output result is severely affected by the parameter selection? If inappropriate parameters are chosen, this can easily cause the iteration process to diverge, which makes it hard to obtain the ideal stochastic-resonance result.

To avoid divergence effectively in the SR iteration process, let us analyze the influence that  $b$  and  $R$  have on the stability of SR.

It can be obtained from Eqs. (1) and (2) that:

$$\begin{aligned} \dot{x} &= ax - bx^3 + s(t) + n(t) \\ &= ax - bx^3 + Sn(t) \end{aligned} \quad (3)$$

Where  $Sn(t)$  is the signal mixed with noise, and a real-world vibration signal has been used.

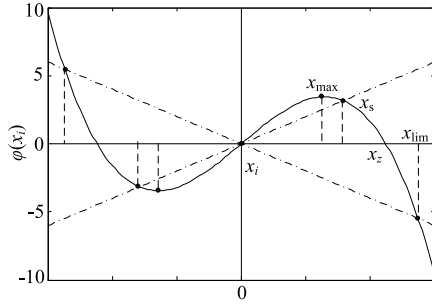


FIGURE 1. Stability region partition of  $\varphi(x)$  curve.

Discretizing the system expressed in Eq. (3) [23],  $h$  is the sampling step of the signal, and  $h = 1/fs$ ; then:

$$\frac{x_{i+1} - x_i}{h} = ax_i - bx_i^3 + Sn_i$$

In other words,

$$x_{i+1} = (1 + ah - bhx_i^2)x_i + hSn_i \quad (4)$$

Under the conditions of the scale-transformation SR algorithm,  $h = 1/fsr = R/fs$ ,

$$\begin{aligned} x_{i+1} &= (1 + \frac{aR}{fs})x_i - \frac{bR}{fs}x_i^3 + \frac{R}{fs}Sn_i \\ &= \varphi(x_i) + \frac{R}{fs}Sn_i \end{aligned} \quad (5)$$

Where  $\varphi(x_i) = (1 + \frac{aR}{fs})x_i - \frac{bR}{fs}x_i^3$ .

Fig. 1 shows the  $\varphi(x_i)$  curve. If when the input signal is  $Sn_i = 0$ , the system will satisfy the following equation after the iteration:

$$x_{i+1} = (1 + \frac{aR}{fs})x_i - \frac{bR}{fs}x_i^3 = x_i \quad (6)$$

By substituting  $x_{i+1}$  into Eq. (6), it can be obtained that  $x_{i+2} = x_{i+1}$ . In a similar way, it is determined that  $x_{i+2} = x_{i+3} = x_{i+4} = x_{i+5} = \dots$ ; then the system reaches a stable state, and the respective value of  $x$  is that of  $x_s$  in Fig.1. The two dot dash lines in Fig.1 are  $y = x$  and  $y = -x$  respectively, while  $x_s$  is the crossover point of  $y = x$  and the  $\varphi(x_i)$  curve, for which the values are  $x_s = \pm\sqrt{a/b}$  and 0.

When

$$1 + \frac{aR}{fs} - \frac{bR}{fs}x_i^2 < -1$$

It can be obtained from Eq. (6) that

$$x_{i+1} = (1 + \frac{aR}{fs} - \frac{bR}{fs}x_i^2)x_i < -x_i \quad (7)$$

Which leads to  $|x_{i+1}| > |x_i|$ ; in a similar way, it can be determined that  $|x_{i+2}| < |x_{i+3}| < |x_{i+4}| < |x_{i+5}| < \dots$ . If the iteration is carried out under this condition, it is certain that  $\lim_{k \rightarrow \infty} |x_{i+k}| = \infty$ , which means that the system must be divergent. Thus, if the system is to be stable, the foremost condition that it must satisfy is:

$$1 + \frac{aR}{fs} - \frac{bR}{fs}x_i^2 > -1 \quad (8)$$

Solving, it can be determined that

$$|x_i| \leq \sqrt{\frac{aR + 2fs}{bR}} = x_{lim} \quad (9)$$

Where  $x_{lim}$  is the crossover point of  $y = -x$  and the  $\varphi(x_i)$  curve in Fig.1.

In Fig.1,  $x_{max}$  is the extreme point of the  $\varphi(x_i)$  curve, while  $x_z$  is its zero point. It can be seen easily that

$$|x_{max}| = \sqrt{\frac{fs + aR}{3bR}}, \quad |x_z| = \sqrt{\frac{fs + aR}{bR}}$$

According to [22],  $x_{max}$  must satisfy the following inequality:

$$|x_{max}| = \sqrt{\frac{fs + aR}{3bR}} \geq |x_s| = \sqrt{\frac{a}{b}} \quad (10)$$

Solving, it can be determined that

$$aR \leq \frac{fs}{2} \quad (11)$$

Where the value of  $x$  is any point in the range determined by Eq. (10).

It can be obtained from Eq. (9) and (11) that the conditions that the SR parameters  $b, R$  need to satisfy are:

$$(b|x_i|^2 - a)R \leq 2fs \text{ and } R \leq fs/2a \quad (12)$$

Furthermore, after deformation,

$$R \leq 2fs/(b|x_i|^2 - a) \text{ and } R \leq fs/2a \quad (13)$$

These inequalities are both used to obtain the range of  $R$ , because  $R$  and  $fs$  are nonnegative.

The following two situations were further investigated:

(1) When  $b > 5a/|x_i|^2$ ,  $2fs/(b|x_i|^2 - a) < fs/2a$ , and Eq. (13) can be expressed as follows:

$$1 \leq R < 2fs/(b|x_i|^2 - a) \quad (14a)$$

where  $R \geq 1$  because the small-parameter change status is assumed in the scale-transformation SR algorithm.

(2) On the contrary, when

$$1 \leq R < fs/2a \quad (14b)$$

Eq. (14) gives the value range in which the SR parameters  $a, b$ , and  $R$  can satisfy the stability conditions.

#### IV. PSO OPTIMIZATION STOCHASTIC-RESONANCE ALGORITHM WITH STABILITY MUTATION OPERATOR

PSO is a global algorithm which is based on the foraging behavior of birds. Compared with the genetic algorithm or the mosquito swarm, this method contains fewer parameters to adjust, which makes it easier to implement and simplifies the algorithm. Because of this, PSO is widely used in various multi-objective optimization problems. Consequently, the PSO algorithm was chosen as the optimization method for the adaptive SR algorithm proposed in this article. However, if the relationship parameters are defined inappropriately, premature optimization and non-convergence problems always emerge [24].

Therefore, if PSO were to be used in the adaptive stochastic-resonance method, the inherent premature optimization and non-convergence problems of PSO would need to be solved first. Even more important, divergence due to inappropriate parameter values would also need to be avoided. To solve these two problems, this paper has proposed a PSO optimization stochastic-resonance algorithm with mutation operator.

#### A. INTRODUCTION OF THE CLASSICAL PSO ALGORITHM

Classical PSO can be expressed as follows: assuming a particle swarm composed of  $m$  particles in a  $D$ -dimensional search space, the location of particle  $i$  is defined as  $X(i) = (x_{i1}, x_{i2}, \dots, x_{iD})$ ,  $i = 1, 2, \dots, m$ , where the optimal position that it has experienced is  $P_i$ , its fitness is  $F_i$ , and its speed is  $V_i$ . The global optimal position is  $P_g$ , which is the optimal position among those experienced by all particles. Then the  $d^{\text{th}}$  dimension of the  $i^{\text{th}}$  particle in generation  $n + 1$  can be calculated iteratively according to the following equations:

$$v_{id}^{n+1} = w \times v_{id}^n + c_1 \times r_1 \times (P_{id}^n - x_{id}^n) + c_2 \times r_2 \times (P_{gd}^n - x_{id}^n) \quad (15)$$

$$x_{id}^{n+1} = x_{id}^n + v_{id}^{n+1} \quad (16)$$

Where  $w$  is inertial weight,  $c_1, c_2$  are acceleration coefficients, which usually have the same value, and  $r_1, r_2$  are two random values in the range  $[0, 1]$ .

In the process of optimization, the speed of the particle is usually limited to a range with  $v_{\max}$  as its critical value, and the position of the particle is also limited within a permitted range. In addition, during the iteration process,  $P_i$  and  $P_g$  will be constantly renewed so that the optimal solution of  $P_g$  can be obtained.

#### B. INERTIAL WEIGHT DEGRESSION STRATEGY BASED ON PARTICLE DISTANCE

One of the universal weaknesses of the classical PSO is its inadequacy in local search, which causes the problem that convergence speed is fast in the early stage, but slow in the later stage, which decreases solution accuracy. According to research, the inertial weight  $w$  in Eq. (15) has a remarkable effect on the global and local search capabilities of the algorithm [25]. This parameter can adjust the speed of the particle dynamically in real time. When the value of  $w$  is large, the particle tends toward global search, and when the value is small, it tends toward local search.

Inspired by this observation, a weight-degression strategy is proposed here. The most widely used weight-degression strategy is the linear decreasing inertial weight (LDIW) strategy, which can be described as follows:

$$\omega = \omega_{\max} - (\omega_{\max} - \omega_{\min}) \times n/n_{\max} \quad (17)$$

where  $\omega_{\max}$  and  $\omega_{\min}$  are the given bounds of the weight,  $n$  is the number of iterations, and  $n_{\max}$  is the maximum number of iterations. It can be seen from Eq. (17) that when using this strategy, the value of  $\omega$  changes linearly and is determined

only by the current number of iterations. With this strategy, the value of  $w$  decreases linearly, and the further the iteration process continues, the smaller the value of  $w$  becomes. Thus, the strategy guarantees that the particle value will not change abruptly near the optimal solution. However, this method ignores the variety of the particle population. If the value of  $\omega$  is decreased at a constant rate in the convergence process, it does not satisfy the requirements of a practical PSO search process, and the solution will be affected to a large degree.

According to [26], when choosing the weight, the position of the particle should be the main concern, and the concept of particle distance is therefore introduced. If the number of iterations is  $n$ , the  $j^{\text{th}}$  dimension of particle  $i$  can be expressed as follows:

$$r_i^n = \frac{1}{d} \sqrt{\sum_{j=1}^d (x_{ij}^n - P_{gj}^n)^2} \quad (18)$$

The larger the value of  $r_i^n$ , the farther the particle is from the global optimal solution, in which case a larger inertial weight should be chosen to reinforce the global search capability.

In fact, the optimal solution search process for PSO can be analyzed as follows: in the initial iterations, the particle is far away from the global optimal solution, which means that a larger inertial weight should be used to guarantee a relatively high particle speed, so that the particle can reach the neighborhood where the optimal solution lies. On the other hand, in the later iterations, the particle is already very close to the global optimal solution, and therefore the inertial weight should maintain a small value to slow down the particle so that local search is performed about the global optimal solution until the convergence conditions are met.

According to this concept, an inertial weight degression strategy based on particle distance is proposed in this paper in accordance with the concept of particle distance. It can be expressed as follows:

$$\omega_i = \omega_{\min} \left( \frac{\omega_{\max}}{\omega_{\min}} \right)^{1 - \frac{r_i^n - r_{\min}^n}{r_{\max}^n - r_{\min}^n}} \quad (19)$$

According to [25], the value range of  $\omega$  is defined as  $[0.4, 0.95]$  to ensure an optimal result from the algorithm. Setting  $r_{\min}^n = 0$ ,  $r_{\max}^n = 10$ , the weighting curve shown in Fig.2 is obtained. It is apparent that the longer the distance between the particle and the optimal solution, the larger  $\left| \frac{r_i^n - r_{\min}^n}{r_{\max}^n - r_{\min}^n} \right|$  is, and according to Eq. (19), when the weight is close to  $\omega_{\max}$ , a powerful global search capability will be achieved. When the particle is close to the optimal solution,  $\left| \frac{r_i^n - r_{\min}^n}{r_{\max}^n - r_{\min}^n} \right|$  will decrease, which enables the particle to perform local search better. The proposed inertial weight degression based on a particle distance index can coordinate effectively the relation between global search and local search. The premature optimization and non-convergence of classical PSO, as well as the low solution accuracy problem, can be overcome to some degree.

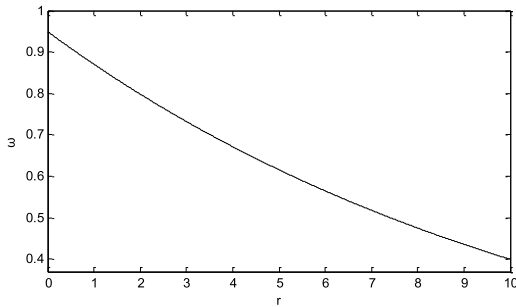


FIGURE 2. Inertial weight change with r.

**C. MUTATION OPERATOR BASED ON STABLE RANGE**

According to the stability analysis results for SR in Section 3, the values of the system parameters  $a$ ,  $b$  and of the frequency compression ratio  $R$  can affect algorithm stability. For PSO, in the initial iteration phase, the randomly generated particles are highly random. The particles' value range changes greatly during the iteration process. The parameter values will probably overstep the stability constraints, which can induce divergence and instability during the iteration process. Based on the stability result presented in Section 3, and inspired by the idea of mutation in a genetic algorithm, a mutation operator based on the stable range is proposed, which will be added to the PSO algorithm. This operator is used to ensure that during the optimal solution search process, no particle will deviate from the normal search range. By setting  $x_i = [b_i, R_i]^T$ , it is possible to obtain the specific mutation process given the input signal:

$$x_i = [b_i, rand[R_l, R_b]]^T + \mu\delta, \quad R_i > R_b \quad (20)$$

where  $R_l$  is the lower bound of  $R$  determined according to the signal feature and  $R_b = \min(2fs/(b_i |x_i|^2 - a), fs/2a)$  is the stability threshold of the current particle corresponding to the frequency compression ratio  $R$ .  $\mu = [\mu_1, \mu_2]$  is the amplitude of the random-disturbance parameter vector. The values of  $\mu_1$  and  $\mu_2$  should be defined as five percent of  $b_i$  and  $R_b$ .  $\delta = [\delta_1, \delta_2]^T$  is the random vector that satisfies a Gaussian distribution whose amplitude is one. Adding  $\mu\delta$  serves to maintain particle variability and to avoid being trapped in a local optimum.

**D. PSO OPTIMIZATION SCALE-TRANSFORMATION STOCHASTIC-RESONANCE ALGORITHM WITH MUTATION OPERATOR**

According to the improved PSO method presented in Section IV part B and C, a PSO optimization algorithm based on stability constraints is proposed in this paper to avoid convergence and stability problems. The algorithm procedure can be described as follows:

*Step 1:* Determine the population scale  $m$  and initialize the position and the bounds of the speed  $v_{max}$ ,  $v_{min}$ , the acceleration coefficients  $c_1$ ,  $c_2$ , and the disturbance coefficients  $r_1$ ,  $r_2$ . Generate the initial population randomly and obtain the position and speed of every particle.

*Step 2:* Calculate the fitness  $F_i$  of particle  $i$ , determine the optimal position  $P_i$  of the particle itself and the global optimization position  $P_g$ . Recalculate the inertial weight  $\omega_i$  of the particle according to Eq. (19) and recalculate the speed and position of the particle.

Here the fitness function chosen is the SNR of the system output signal, for which the calculation formula is [7]:

$$SNR = 10 \lg \frac{S(f_0)}{N(f_0)} = 10 \lg \frac{|Y(f_0)|^2}{N(f_0)} \quad (21)$$

Where  $S(f_0)$  is the amplitude of the output power spectrum  $Y(f_0)$  when the system generates an output signal of frequency  $f_0$ . The background noise  $N(f_0)$  is the average value in the frequency range when the frequency of  $Y(f_0)$  is  $f_0$ . When the output SNR reaches the maximum value, the SR is in the best state. Therefore, the SNR can be the fitness function of the PSO algorithm.

*Step 3:* Check whether the position of particle  $i$  can satisfy the calculated stability conditions. When  $R_i > R_d$ , perform the mutation operation  $x_i$  according to Eq. (20), generate a new population, and move to STEP 4; when  $R_i \leq R_d$ , this means that the particle satisfies the stability conditions, so move to STEP 4 directly.

*Step 4:* Evaluate whether the stopping condition has been satisfied. If so, output the current  $P_g$  and terminate the algorithm because the optimal particle that satisfies the conditions has been obtained; if not, return to STEP 2.

**V. NUMERICAL SIMULATION ANALYSIS AND EXPERIMENTAL VERIFICATION**

**A. ANALYSIS OF LARGE-PARAMETER NUMERIC SIGNALS**

Define the input signal as:

$$Sn(t) = A \sin(2\pi ft) + \sqrt{2D}\xi(t) \quad (22)$$

To simulate large-parameter conditions, the parameters in Eq. (21) were selected as  $A = 0.5$ ,  $f = 10$ ,  $D = 10$ , the sampling frequency was set to 2000 Hz, and the data length was 20000 points. According to the design concept of the proposed algorithm, the system parameter  $a$  was set to one, and the search range of  $a$  was [1, 20]. Then Eq. (14) defines the value range of  $R$ . During the computation process, particles that fail to satisfy the stability conditions will mutate based on Eq. (20). Fig. 3 shows the time-domain waveform and amplitude spectrum of the original signal. Fig. 4 shows the analytical results of the classical PSO optimization SR algorithm, and Fig. 5 shows the analytical results of the proposed PSO optimization SR algorithm. For the sake of convenience, the classical PSO optimization SR algorithm will be called the classical PSO-SR algorithm, and the PSO optimization scale-transformation stochastic-resonance algorithm with mutation operator will be called the proposed PSO-SR algorithm if not further qualified.

According to Fig.3, the designed simulation signal satisfies the large-parameter conditions. Under the influence of noise, the time-domain signal is entirely disordered, and the feature frequency is indistinguishable in the frequency-domain

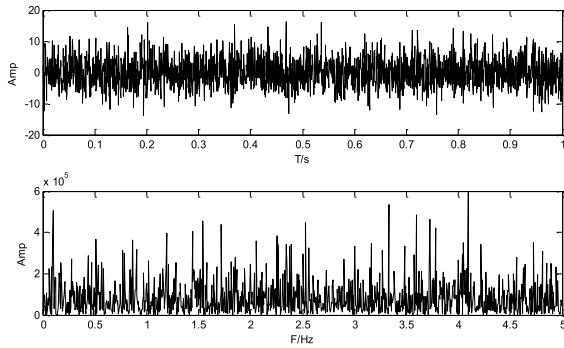


FIGURE 3. Time-domain waveform and amplitude spectrum of the original numerical signal.

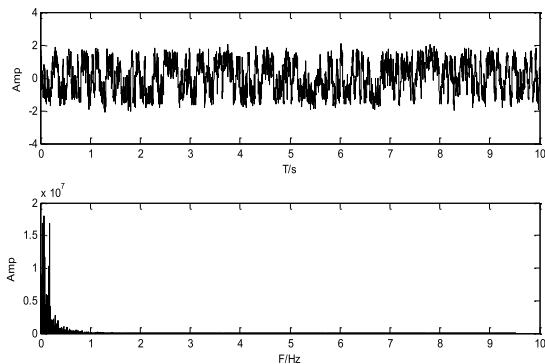


FIGURE 4. Signal-processing result of the classical PSO-SR algorithm.

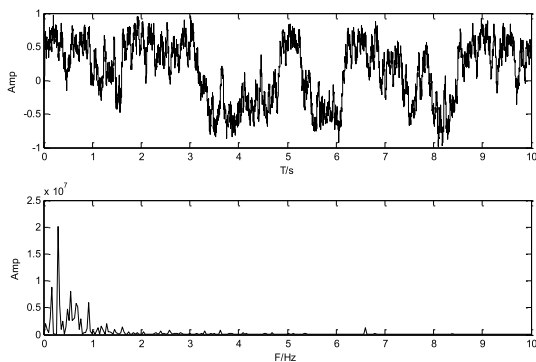
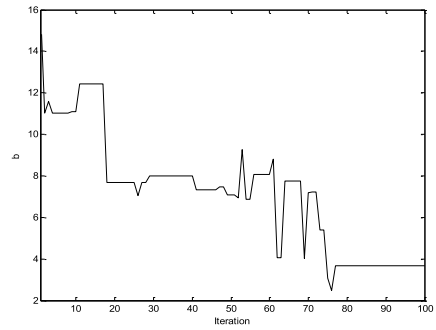


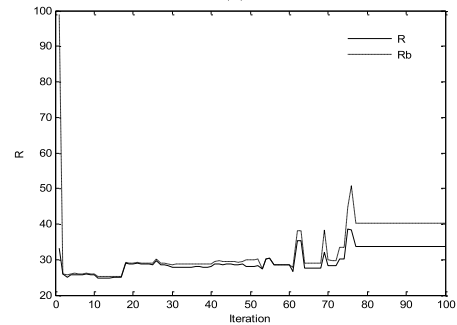
FIGURE 5. Signal-processing result of the proposed PSO-SR algorithm.

curve. However, the time-domain signal in Fig.4 shows a periodic character. Three obvious peaks can be seen in the low-frequency area, with values of 0.04591, 0.07322, and 0.1906 Hz respectively, where the frequency compression ratio  $R$  is 53.2659. The real values of these frequencies can be reverted according to Section 1.2 to yield values of 2.4454, 3.9001, and 10.1525 Hz respectively. It is obvious that the first two frequencies have nothing to do with the given signal, that is, that they are useless low-frequency values, and that the third frequency corresponds to the signal feature frequency.

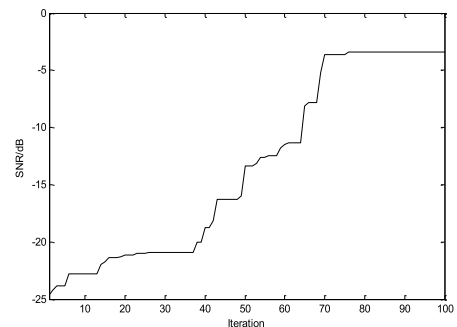
According to SR theory, the signal power is diverted to the low-frequency range, which is driven by noise (the Lorentz



(a)



(b)



(c)

FIGURE 6. Optimization results of the proposed PSO-SR algorithm.

effect). As a result, some inconspicuous frequency components will appear. The result in Fig. 4 was induced by an oversized  $R$  value. Because the dereferencing process is unrestricted in the traditional PSO algorithm, an inappropriate  $R$  value was obtained. Then the signal power is diverted too strongly to the low-frequency range, and some low-frequency components mixed in with the signal are enhanced and appear.

Fig.6 shows the analytical results of the algorithm proposed in this article. The iteration process ended at the 77<sup>th</sup> generation. The optimal solution values were  $b_{best} = 3.6559$  and  $R_{best} = 33.7284$ , and the feature frequency in Fig.5 was 0.2971 Hz. The evolution processes of parameters  $b$  and  $R$  are shown in Fig.6(a) and 6(b) respectively. Fig.6(c) shows the change in the output SNR during the optimization process. From Fig.6(b), the frequency compression ratio  $R$  clearly remained inside the constraint range for a stable condition. This suggests that the mutation operator worked. Consequently, the stability of the parameter optimization process

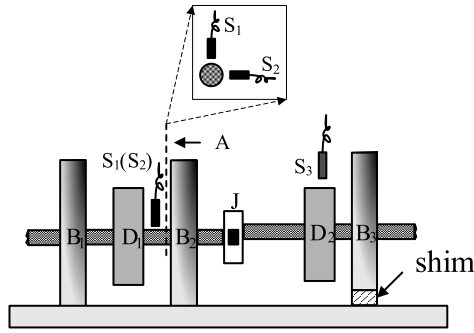


FIGURE 7. Sketch of the misalignment fault simulation.

can be guaranteed, and the result overflow problem has been avoided. The output SNR increased from  $-24.6158dB$  to  $-3.3868dB$ . According to scale-transformation SR theory, the feature frequency could be reverted to  $f_c = 33.7284 \times 0.2971 = 10.0207dB$ , which corresponds to the original signal. These results show that the algorithm proposed in this article is competent for detecting large-parameter signals.

**B. VIBRATION SIGNAL ANALYSIS OF ROTOR MISALIGNMENT FAULT**

To verify the functioning of the proposed algorithm with real engineering signals, a birotor test table was used for an early fault-simulation test. The test table consisted of a foundation bed, electric motor, axle trees, bearings, coupling, turntable, and other components. The rotors were carried on sliding bearings and driven by a direct-current electric motor. The rotational speed ranged from 0 to 15000 rpm. The electric motor and rotors were connected by flexible couplings, which provided vibration flexibility in the crosswise direction. Fig. 7 shows a sketch of the misalignment-fault simulation, where  $B_i(i = 1, \dots, 3)$  are bearing tables and  $D_i(i = 1, 2)$  are turntables.  $S_1, S_2$  are vibration sensors; they are eddy-current sensors and located in orthogonal directions, which enables them to test the vibration displacement of rotors.  $S_3$  is used to test the rotation-speed sensor, which is a photoelectric speed sensor.  $J$  is a coupling, and  $S_1$  is an electric eddy-current sensor which can measure the vibration displacement in the horizontal and vertical directions of the measurement point above.

Misalignment faults are a common fault in rotor systems [27]. In rotary machines with dual or multiple rotors, the rotors are connected by couplings. However, during manufacturing, installation, or operation, asymmetrical excursions or deformations always occur in bearing systems. Then parallel misalignment, angle misalignment, or both will occur in the couplings. To simulate a misalignment fault, a shim was inserted into the bottom of one bearing on one side. A deviation was thus induced between the two sides of the coupling  $J$ , and a misalignment fault resulted. In general, radial vibration is strongest when a misalignment fault is present. The  $2X$  frequency components are the primary feature, which are always coupled with  $1X$  and  $3X$  components, but the  $2X$  components are stronger than any others.

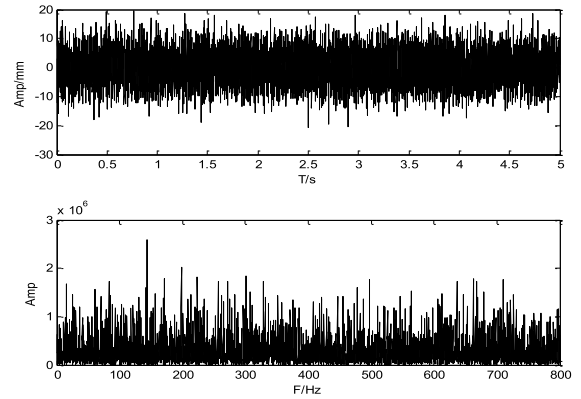


FIGURE 8. Time-domain waveform and amplitude spectrum of misalignment fault.

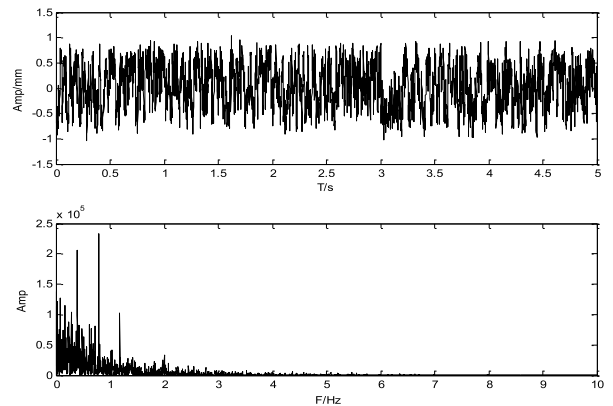


FIGURE 9. Result of processing by classical PSO-SR algorithm.

The electric motor speed was set to 1500 r/min, which meant that the rotor working frequency was 25 Hz. The sensor sampling frequency was 200 Hz, and the sampling time was 5 s. The vibration signal in the vertical direction is analyzed here. Fig. 8 shows the time-domain waveform and amplitude spectrum of the input signal. The time-domain waveform is completely disordered, with the signal feature drowned by strong noise. Hardly any effective fault information can be obtained. The frequency spectrum is also irregular, and no regularity can be found to ascertain faults. Irregular peaks appear in all frequency ranges.

Fig.9 and Fig.10 show the output results of the classical PSO-SR algorithm and the PSO-SR algorithm respectively. The feature frequency was detected by both algorithms. The highest peak in Fig.9 corresponds to a frequency of 0.7563 Hz. The frequency compression ratio  $R = 66.2561$ . The feature frequency could be reverted as  $f_c = 50.1095Hz$ . In a similar way, the feature frequency in Fig.8 can be obtained as  $f_{c0} = 0.7909 \times 63.4702 = 50.1986Hz$ . These two feature frequencies are both  $2X$  the working frequency. At the same time, another two obvious frequencies in Fig. 9 are 0.3778Hz and 1.1298Hz, and the corresponding actual frequencies are 25.0316Hz and 74.8561Hz. These are the  $1X$  and  $3X$  frequency components of the rotor system. In conclusion, the frequency analysis results



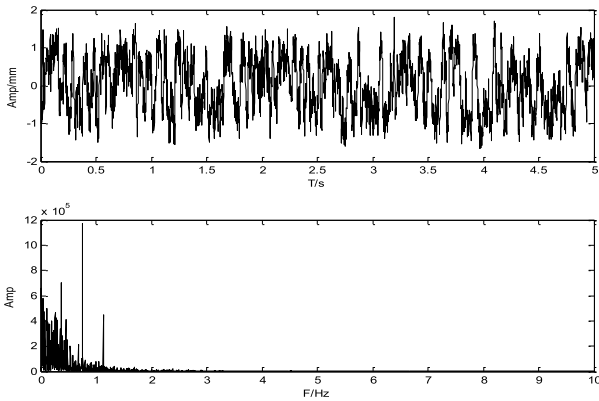


FIGURE 10. Result of processing by proposed PSO-SR algorithm.

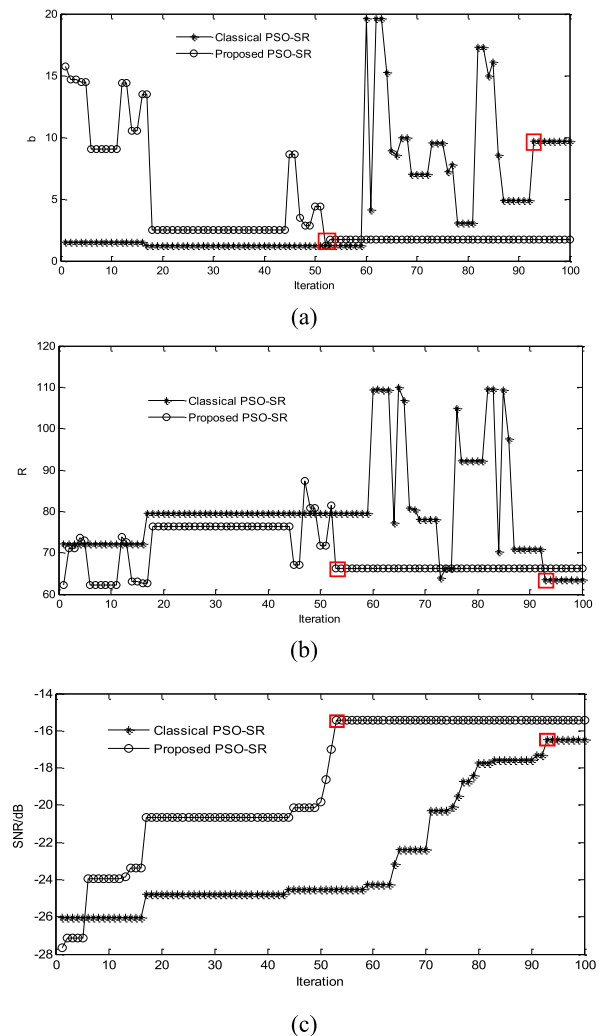


FIGURE 11. Curve of the parameter optimization process.

correspond with the frequency features of the misalignment fault.

Fig. 11 shows the optimization process for the two methods. Fig. 11(a) illustrates the optimization process of parameter  $b$ ,

TABLE 1. Computed optimization results.

Parameter	Classical PSO-SR Algorithm	Proposed PSO-SR Algorithm
$b$	9.7116	1.7438
$R$	63.4702	66.2561
SNR	-16.5365	-15.4354

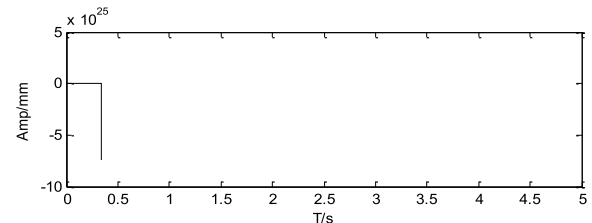


FIGURE 12. Overflow phenomenon in the classical PSO-SR algorithm.

Fig. 11(b) shows the optimization process of parameter  $R$ , and Fig. 11(c) illustrates the changes in the output SNR.

The classical PSO-SR algorithm and the proposed PSO-SR algorithm reach stable status in generation 93 and generation 53 respectively. Some key parameters of stable status are shown in Table 1. Because  $b$  and  $R$  have been selected as the optimization parameters, optimization by the PSO algorithm will produce many different combinations. Moreover, the parameters of the classical algorithm exhibit more severe changes. Especially in the later iteration stage, because the inertial weight is uncontrollable, the parameter optimization process does not proceed in an acceptable neighborhood of the optimal solution. This situation makes the parameter convergence process excessively slow. However, the proposed algorithm introduces the inertial weight convergence strategy based on particle distance and a stable mutation operator. The former sets  $\omega$  to a smaller value in the later iteration stage, which will make the particle perform local search near the optimal solution. The latter restricts the value of  $R$ . If a particle does not satisfy the stable condition, the mutation operator will go to work immediately. Thus, the situation in which the particle moves outside the stable range will be avoided. Stability is guaranteed during the whole optimization process, and the optimal solution can be reached more quickly.

After testing, it was found that overflow phenomena always occur in the classical PSO-SR algorithm, and the iteration stops prematurely. The time-domain data can be obtained in the MATLAB workspace. Fig. 12 shows the time-domain waveform.

## VI. CONCLUSIONS

With a focus on certain problems with the SR algorithm (difficulty of parameter selection, keeping the calculation from diverging), a PSO optimization scale-transformation stochastic-resonance algorithm with mutation operator has

been proposed in this paper. The results showed that when the stable mutation operator acted on the SR optimization parameters, divergence was effectively avoided, and the stability of the iterative algorithm was improved accordingly. By adding the inertial weight degression strategy to the PSO algorithm, the iteration speed was improved at the same time.

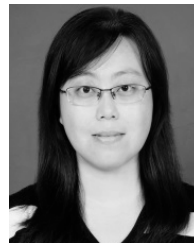
When using the method described in this paper for signal processing, the authors found that differences in the noise intensity of the original signal could possibly lead to differences in the optimization parameters. Focusing on this phenomenon, further research will explore how to determine the appropriate pretreatment method according to the features of the signal and how to filter out noise and certain irrelevant frequencies so that algorithm accuracy can be further increased.

### ACKNOWLEDGMENTS

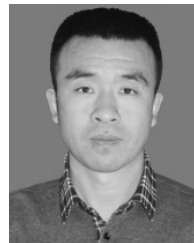
The authors would like to thank the anonymous reviewers for their valuable comments and suggestions.

### REFERENCES

- [1] W. Chen, L. Cheng, and Q. T. Li, *Monitoring Technology of Aero-Engines*. Beijing, China: National Defence Industry Press, 2010.
- [2] R. Benzi, A. Sutera, and A. Vulpiana, "The mechanism of stochastic resonance," *J. Phys. A, Math. Gen.*, vol. 14, no. 11, pp. 453–457, 1981.
- [3] Y. G. Leng, "Mechanism analysis of the large signal scale-transformation stochastic resonance and its engineering application study," School Mech. Eng., TianJin Univ., Tianjin, China, Tech. Rep., 2004.
- [4] J. Li, X. Chen, and Z. He, "Adaptive stochastic resonance method for impact signal detection based on sliding window," *Mech. Syst. Signal Process.*, vol. 36, no. 2, pp. 240–255, 2013.
- [5] Q. He, J. Wang, Y. Liu, D. Dai, F. Kong, "Multiscale noise tuning of stochastic resonance for enhanced fault diagnosis in rotating machines," *Mech. Syst. Signal Process.*, vol. 28, pp. 443–457, Apr. 2012.
- [6] N. Hu, M. Chen, and X. Wen, "The application of stochastic resonance theory for early detecting rub-impact fault of rotor," *Mech. Syst. Sig. Process.*, vol. 17, no. 4, pp. 883–895, 2003.
- [7] A. S. Asdi and A. H. Tewfik, "Detection of weak signals using adaptive stochastic resonance," in *Proc. IEEE Int. Conf. Acoust., Speech, Signal Process.*, May 1995, pp. 1332–1335.
- [8] S. Mitaim and B. Kosko, "Adaptive stochastic resonance," *Proc. IEEE*, vol. 86, no. 11, pp. 2152–2183, Nov. 1998.
- [9] Q. Ye, H. Huang, X. He, and C. Zhang, "A study on the parameters of bistable stochastic resonance systems and adaptive stochastic resonance," in *Proc. IEEE*, Oct. 2003, pp. 484–488.
- [10] X. L. Yang et al., "Adaptive stochastic resonance technology in detecting weak signal," *Signal Process.*, vol. 25, no. 1, pp. 8–10, 2004.
- [11] X. Deng et al., "Study on self-adopting scanning to stochastic resonance," *J. Xi'an Jiaotong Univ.*, vol. 39, no. 1, pp. 108–110, 2005.
- [12] W. L. Zhao and L. H. Guo, "Stochastic resonance and adaptive signal detection," *J. Electron. Meas. Instrum.*, vol. 20, no. 5, pp. 21–25, 2006.
- [13] X. Yi, W. Rui, and W. Fei, "Detection of amplitude-varied weak signal by genetic adaptive stochastic resonance algorithm," in *Proc. IEEE*, Aug. 2007, pp. 626–630.
- [14] Q. Huang, J. Liu, and H. Li, "A modified adaptive stochastic resonance for detecting faint signal in sensors," *Sensors*, vol. 7, no. 2, pp. 157–165, 2007.
- [15] J. Tan, X. Chen, and Z. He, "Adaptive frequency-shifted and re-scaling stochastic resonance with applications to fault diagnosis," *J. Xi'an Jiaotong Univ.*, vol. 43, no. 7, pp. 69–73, 2009.
- [16] W. Shen, Q. Pang, and Y. L. Fan, "Study on strong noise image restoration based on adaptive stochastic resonance in bistable system," *Comput. Eng. Appl.*, vol. 45, no. 15, pp. 180–182, 2009.
- [17] D. Wu, S. Zhu, X. Luo, and L. Wu, "Effects of adaptive coupling on stochastic resonance of small-world networks," *Phys. Rev. E*, vol. 84, no. 2, p. 021102, 2011.
- [18] J. Wang et al., "Adaptive stochastic resonance based on genetic algorithm with applications in weak signal detection," *J. Xi'an Jiaotong Univ.*, vol. 44, no. 3, pp. 32–36, 2010.
- [19] L. P. Wu, Z. Li, and J. D. Li, "Analysis on stochastic resonance parameters adaptive adjusting," *J. Beijing Univ. Posts Tel.*, vol. 34, no. 2, pp. 21–22, 2011.
- [20] B. Li, J. Li, and Z. He, "Fault feature enhancement of gearbox in combined machining center by using adaptive cascade stochastic resonance," *Sci. China/Technol. Sci.*, vol. 54, no. 12, pp. 3203–3210, Dec. 2011.
- [21] J. Li, X. Chen, and Z. He, "Adaptive monostable stochastic resonance based on PSO with application in impact signal detection," *J. Mech. Eng.*, vol. 47, pp. 58–63, 2011.
- [22] D. X. Yang, "On methodology and application of weak characteristic signal detection based on stochastic resonance," College Mechatronics Eng. Autom., Nat. Univ. Defense Technol., Changsha, China, Tech. Rep., 2004.
- [23] N. Hu, M. Chen, G. Qin, L. Xia, Z. Pan, and Z. Feng, "Extended stochastic resonance (SR) and its applications in weak mechanical signal processing," *Frontiers Mech. Eng. China*, vol. 4, p. 450, Dec. 2009.
- [24] G. Xu, Z. P. Qu, and Z. T. Wang, "Improved adaptive particle swarm optimization algorithm," *J. South China Univ. Technol. (Natural Sci. Ed.)*, vol. 45, no. 2, pp. 402–409, 2008.
- [25] Y. Shi and R. C. Eberhart, "Empirical study of particle swarm optimization," in *Proc. CEC*, Jul. 1999, pp. 1945–1950.
- [26] G. Chen, J. Jia, and Q. Han, "Study on the strategy of decreasing inertia weight in particle swarm optimization algorithm," *J. Xi'an Jiaotong Univ.*, vol. 40, no. 1, pp. 53–61, 2006.
- [27] B. C. Wen, X. H. Wu, Q. Ding, *The Nonlinear Dynamics Theory and Test of Fault Rotating Machine*. Beijing, China: Science Press, 2004.



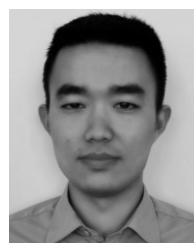
**LING TONG** was born in 1977. She received the master's degree in computer application technology from Xidian University in 2010. She is currently a Lecturer. Her main research interests include process control and data mining. She has authored three papers in Chinese and English version of the *Acta Aeronautica Et Astronautica*.



**XIAOGANG LI** was born in 1977. He received the master's degree from the Aeronautics and Astronautics Engineering Institute, Air Force Engineering University, in 2007. He is currently an Associate Professor. His main research interests include aircraft fluid transmission and control.



**JINHAI HU** was born in 1978. He received the Ph.D. degree from the Aeronautics and Astronautics Engineering institute, Air Force Engineering University in 2007. He is currently an Associate Professor. He has authored over 40 papers in Chinese and English version of the *Acta Aeronautica Et Astronautica*. His main research interests include aeroengine control and condition monitoring.



**LITONG REN** was born in 1987. He is currently pursuing the Ph.D. degree with the Aeronautics and Astronautics Engineering Institute, Air Force Engineering University. His main research interests include distributed control system and sliding mode control.

...